Taming the coil: stabilizing a model hemoprotein fold *via* macrocyclization and peptide helix capping

Dahui Liu, Kyung-Hoon Lee and David R. Benson*

Department of Chemistry, University of Kansas, Lawrence, KS 66045-0046, USA.
E-mail: dbenson@caco3.chem.ukans.edu

Received (in Columbia, MO, USA) 16th February 1999, Accepted 17th May 1999

An N-terminal helix capping motif combined with a C-terminal disulfide bridge stabilizes the fold of a designed hemoprotein model.

Structural stability of many proteins is enhanced by disulfide bonds[1] or by coordination of metal ions to groups of amino acid side chain ligands.[2] Induction of helicity in short peptides has also been accomplished using these and other side chain-side chain interactions.[3] Employing a related approach, we achieved moderate helix induction upon histidine (His) to iron coordination in covalent peptide–porphyrin adducts known as peptide-sandwiched mesohemes (PSMs).[4] Similar helix induction was obtained in a disulfide-dimerized peptide upon complexation of a cobalt(III) porphyrin.[5] To aid our goal of creating small hemoprotein mimics having protein-like stability, we have been exploring ways to further reduce peptide conformatioal flexibility in our designs. The successful use of aromatic side chain–porphyrin interactions in the PSMs has recently been reported.[6]

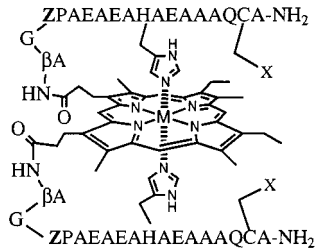

A = Ala; C = Cys; E = Glu; G = Gly; H = His; Q = Gln; P = Pro

1 X,X = S–S; Z = Asn; M = Fe^{III}
2 X = SAcm; Z = Asn; M = Fe^{III}
3 X = SAcm; Z = Gln; M = Fe^{III}
4a,b X,X = S–S; Z = Asn; M = Co^{III}

Herein we report preliminary results with **1**, in which extraordinarily high helix content is achieved through a combination of Fe–His coordination, an N-terminal helix capping motif, and macrocyclization *via* disulfide bond formation.

Lack of hydrogen bonding partners for the first and last few amino acids in a peptide helix results in fraying at each terminus.[7] Protein helices often terminate with a capping motif, which reduces the number of unsatisfied hydrogen bonding sites.[8] In the capping box motif, an amino acid with a hydrogen-bond acceptor on its side chain is situated prior to the first N-terminal helical residue. The side chain of this Ncap hydrogen bonds to the backbone amide NH of the third residue in the helix (N3), which otherwise would not have a hydrogen bonding partner other than water. The side chain of N3 (commonly glutamic acid; Glu) reciprocates by hydrogen-bonding to the backbone amide of the Ncap. The importance of side chain entropy in this end-cap motif is highlighted by the fact that asparagine (Asn) is one of the best Ncap residues in peptides while glutamine (Gln) is one of the worst.[9]

One of the most common amino acids at the first position (N1) of protein helices is proline (Pro).[10] Pro is especially useful at N1 as its backbone ϕ angle (which is ideal for residing in a helix) is fixed by its cyclic structure. Lack of a backbone amide hydrogen further works in favor of Pro at N1, as it needs no hydrogen bonding partner.

Based on the above considerations, Asn, Pro and Glu were selected as the Ncap, N1 and N3 residues in the design of **1**. The backbone torsional angles of Asn were set at the average values observed for Ncap residues in natural proteins (ϕ = −94°; ψ = 167°),[8] while the side chain torsional angles of the His residue coordinated to iron mesoporphyrin IX (MP-IX) were set at the favorable combination χ_1/χ_2 = 180°/−90°.[4,11] When His adopts this combination the peptide helix axis lies at an angle of *ca.* 30° relative to the porphyrin plane and the sulfhydryl group of a cysteine (Cys) residue located i + 7 from His is level with the porphyrin edge and just beyond it.[5] Separating Pro and His by five helical amino acids directed the α-amine of Asn toward the propionate groups of MP-IX, while the sequence β-alanine-glycine (β-Ala-Gly) nicely bridged the gap between the two. When a second peptide was incorporated on the other side of MP-IX, the two Cys residues were situated within bonding distance of one another. Fig. 1 shows a predicted energy minimized structure of **1**.[12]

The bis acetamidomethyl (Acm) protected precursor of **1** (**2**) serves to show how the disulfide linkage in **1** influences its structure and stability. We also prepared an analogue of **2** in which the Ncap Asn has been replaced by Gln (**3**) in order to determine whether Asn functions as intended in our design. Syntheses of **2** and **3** were accomplished using methods previously reported for the PSMs.[4] Brief treatment of **2** with iodine in aqueous 2,2,2-trifluoroethanol (TFE) cleanly yielded **1**.

Circular dichroism (CD) spectra of **1**–**3** are shown in Fig. 2. Using the mean residue ellipticity at 220 nm (θ_{220}) we calculate[13] that the peptides in **2** are 64% helical in aqueous solution at 8 °C (Table 1; only amino acids 4–18 are included in the calculation, as only these residues are predicted to be within the helix). In contrast, helix content in **3** is only 45% in water. The high helicity of acyclic **2** supports the choice of His placement in the peptide sequence, while the results with **3** confirm a helix-stabilizing role for the Ncap Asn. The helix stabilizing solvent TFE increases helix contents of **2** and **3** to 88 and 83%, respectively (Table 1). Finally, comparing spectra of **1** and **2** in H_2O (Fig. 2; Table 1) reveals that macrocyclization strongly increases peptide helix content as predicted. TFE

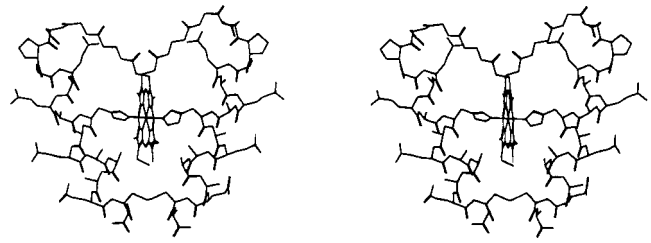

Fig. 1 Structure of one diasteromer of **1** predicted from molecular modeling studies.

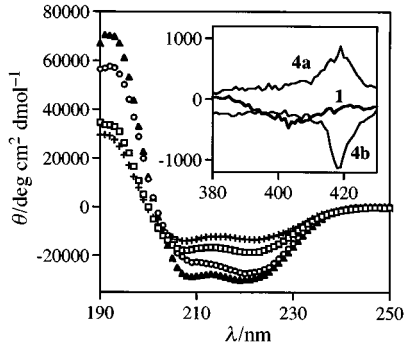

Fig. 2 Far-UV CD spectra of **1** in H_2O (○) and 3:1 (v/v) H_2O–TFE (▲) and of **2** (□) and **3** (+) in H_2O. Inset: Soret region spectra of **1**, **4a** and **4b** in H_2O. All samples were buffered at pH 7.0 with 2 mM potassium phosphate and all spectra were recorded at 8 °C.

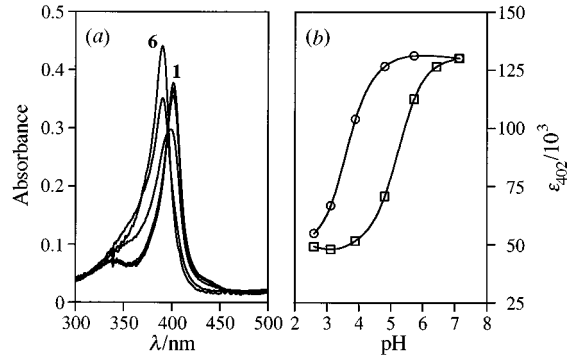

Fig. 3 (*a*) UV/vis spectra of **1** recorded as a function of pH. Spectrum 1: pH 7.1; Spectrum 6: pH 2.6. (*b*) Plots of extinction coefficient (ε) at Soret λ_{max} *vs.* pH for **1** (○) and **2** (□). All data were recorded at 22 °C.

Table 1 CD data for **1**–**4** in H_2O and in 3:1 (v/v) H_2O–TFE

	θ_{220}/deg cm² dmol^{-1} [a] (% Helix)[b]	
Compound	H_2O	3:1 (v/v) H_2O–TFE
1	−27 400 (94)	−30 000 (102)
2	−18 700 (64)	−25 800 (88)
3	−13 300 (45)	−24 000 (83)
4a	−25 500 (87)	−27 800 (95)
4b	−27 800 (95)	−30 100 (102)

[a] θ_{max} = −29 300 deg cm² dmol^{-1}. [b] Percent helix values are shown in parentheses.

further increases helix content in **1** from 94% to the theoretical maximum, although the relative intensities of the 208 and 220 nm bands in the two solvents suggest that TFE may cause additional changes to the structure of **1**.

The heme chromophore can contribute ellipticity in the far-UV region of CD spectra of hemoproteins and hemoprotein models.[14] Calculated helix contents reported in Table 1 must therefore be considered estimates only. Nonetheless, because the chromophore and the mode of attachment of peptide to porphyrin are the same in **1**–**3**, it is reasonable to assume that an increase in the absolute value of θ_{220} represents a proportional increase in peptide helix content.

PSMs built from MP-IX exist in two interconvertible diastereomeric forms.[4] Pavone and co-workers have reported that the two diastereomers of bis-His coordinated hemoprotein models constructed from Co^{III} deuteroporphyrin IX can be separated because His–Co^{III} bonds are exchange-inert.[15] We thus prepared and isolated the two diastereomers of the Co^{III} analogue of **1** (**4a** and **4b**). Helix contents of **4a** and **4b** are different, although both are very high. The CD Soret bands of **4a** and **4b** are of opposite sign but nearly equal intensity, whereas the Soret band of **1** is negative (Fig. 2, inset). That the helix contents of **1** and **4b** are nearly identical (and greater than **4a**) and each exhibits a negative Soret suggests that the diastereomer of **1** which corresponds to **4b** predominates at equilibrium. The diastereomer of **1** shown in Fig. 1 is the one predicted to be favored based on molecular modeling studies.

The intramolecular His ligands in **1**–**3** result in Fe–His coordination being strongly favored at neutral pH. However, because Fe–His bonds are exchange labile, at pH values near or below the pK_a of His, protonation of His competes with Fe–His coordination.[4] Protonation of His requires initial scission of the Fe–His bond, which results in conversion of heme from the low spin (S = 1/2; Soret λ_{max} = 402 nm) to the high spin (S = 5/2; Soret λ_{max} = 390 nm) form. One of our predictions with **1** was that the disulfide bridge would stabilize the folded (bis-His coordinated) form of the molecule relative to **2** by reducing the conformational freedom of its peptides in the unfolded form. We thus recorded UV/vis spectra of **1** and **2** in water as a function of pH (Fig. 3). For **2**, spectral changes are observed at pH values as high as 6. No changes were observed in UV/vis spectra of **1**, however, until pH < 5, illustrating the predicted stability enhancement of bis-His coordinated **1**.

In conclusion, we have shown that a combination of motifs commonly encountered in protein structures can provide considerable structural stabilization to hemoprotein models built from short peptides. The results illustrate the power of computer-aided *de novo* design in creating protein mimics having desired structural characteristics. Future work will be aimed at systematically investigating the influence of the Ncap, N1 and N3 residues in **1** and **2** on the stability of the folded form of each molecule. We also plan a detailed study of the three-dimensional structures of **4a** and **4b** using ^{1}H NMR, which will include an examination of how TFE influences peptide architecture.

This work was supported by NIH grant R29-GM52431.

Notes and references

1 T. E. Creighton, *BioEssays*, 1988, **8**, 57.
2 J. P. Glusker, *Adv. Protein Chem.*, 1991, **42**, 1.
3 J. C. Phelan, N. J. Skelton, A. C. Braisted and R. S. McDowell, *J. Am. Chem. Soc.*, 1997, **119**, 455 and references therein.
4 P. A. Arnold, D. R. Benson, D. J. Brink, M. P. Hendrich, G. S. Jas, M. L. Kennedy, D. T. Petasis and M. Wang, *Inorg. Chem.*, 1997, **36**, 5306.
5 P. A. Arnold, W. R. Shelton and D. R. Benson, *J. Am. Chem. Soc.*, 1997, **119**, 3181.
6 D. A. Williamson and D. R. Benson, *Chem. Commun.*, 1998, 961.
7 A. Chakrabartty and R. L. Baldwin, *Adv. Protein Chem.*, 1995, **46**, 141.
8 E. T. Harper and G. D. Rose, *Biochemistry*, 1993, **32**, 7605; A. J. Doig, M. W. MacArthur, B. J. Stapley and J. M. Thornton, *Protein Sci.*, 1997, **6**, 147.
9 A. J. Doig, A. Chakrabartty, T. M. Klinger and R. L. Baldwin, *Biochemistry*, 1994, **33**, 3396.
10 J. S. Richardson and D. C. Richardson, *Science*, 1988, **240**, 1648.
11 P. Chakrabarti, *Protein Eng.*, 1990, **4**, 57.
12 SYBYL molecular modeling software ver. 6.01, Tripos Associates, St. Louis, MO.
13 P. C. Lyu, J. C. Sherman and N. R. Kallenbach, *Proc. Natl. Acad. Sci. U.S.A.*, 1991, **88**, 5317.
14 D. R. Benson, B. R. Hart, X. Zhu and M. B. Doughty, *J. Am. Chem. Soc.*, 1995, **117**, 8502 and references therein.
15 G. D'Auria, O. Maglio, F. Nastri, A. Lombardi, M. Mazzeo, G. Morelli, L. Paolillo, C. Pedone and V. Pavone, *Chem. Eur. J.*, 1997, **3**, 350.

Communication 9/01312A